AEDC-TR-69-195

PRELIMINARY INVESTIGATION OF THE INTERACTION OF 0.30- TO 0.54-EV GASEOUS ARGON WITH A SOLID ARGON SURFACE

M. R. Busby and R. F. Brown

ARO, Inc.

November 1969

AEROSPACE ENVIRONMENTAL FACILITY
ARNOLD ENGINEERING DEVELOPMENT CENTER
AIR FORCE SYSTEMS COMMAND
ARNOLD AIR FORCE STATION, TENNESSEE

NOTICES

When U. S. Government drawings specifications, or other data are used for any purpose other than a definitely related Government procurement operation, the Government thereby incurs no responsibility nor any obligation whatsoever, and the fact that the Government may have formulated, furnished, or in any way supplied the said drawings, specifications, or other data, is not to be regarded by implication or otherwise, or in any manner licensing the holder or any other person or corporation, or conveying any rights or permission to manufacture, use, or sell any patented invention that may in any way be related thereto.

Qualified users may obtain copies of this report from the Defense Documentation Center.

References to named commercial products in this report are not to be considered in any sense as an endorsement of the product by the United States Air Force or the Government.

PRELIMINARY INVESTIGATION OF THE INTERACTION OF 0.30- TO 0.54-EV GASEOUS ARGON WITH A SOLID ARGON SURFACE

M. R. Busby and R. F. Brown
ARO, Inc.

FOREWORD

The research presented in this report was sponsored by the Arnold Engineering Development Center (AEDC), Air Force Systems Command (AFSC), Arnold Air Force Station, Tennessee, and is related to Program Element 61102F, Project 8951.

The results of research were obtained by ARO, Inc. (a subsidiary of Sverdrup & Parcel and Associates, Inc.), contract operator of the AEDC, AFSC, under Contract F40600-69-C-0001. The research was conducted from October to November 1968 under ARO Project SW3904. The manuscript was submitted for publication on August 4, 1969.

The authors wish to thank Dr. J. D. Haygood, ARO, Inc., and Dr. R. E. Stickney, Massachusetts Institute of Technology, for their suggestions and aid in interpretation of the data.

This technical report has been reviewed and is approved.

Michael G. Buja
2d Lt, USAF
Research Division
Directorate of Plans
and Technology

Harry L. Maynard
Colonel, USAF
Director of Plans
and Technology

ABSTRACT

An aerodynamic molecular beam and phase-sensitive detection system were used to investigate the spatial distributions of argon atoms reflected from solid argon for incident energies of from 0.30 (beam temperature of 1400°K) to 0.54 ev (beam temperature of 2500°K), incident angles from 0 to 70 deg, and solid argon temperatures of 15°K. Both in-plane and out-of-plane spatial distribution measurements were made, and highly nondiffuse supraspecular spatial flux distributions were observed for the noncondensing atoms. The angle of maximum reflected intensity was independent of both beam incident angle and beam energy. For incident angles (measured with respect to the surface normal) of 5 deg or less, "backward" reflection lobes were observed, and the magnitude of the reflected flux increased as the angle of incidence approached zero. The beam capture coefficient was a function of the incident beam energy and the angle of incidence. However, with a beam source temperature of 2500°K, the capture coefficient was near unity for normal incidence.

CONTENTS

APPENDIXES

I. ILLUSTRATIONS

Figure

NOMENCLATURE

A	Maximum signal intensity for cosine distribution
C_b	Beam capture coefficient
I	Beam intensity, molecules/sec-cm^2
m_g	Mass of gas molecule
$\dot{n}_i$	Total incident beam flux, molecules/sec
$\dot{n}_r$	Total reflected beam flux, molecules/sec

$\dot{n}_t$	Total gas flux leaving the surface, molecules/sec
$\dot{n}_v$	Evaporation flux, molecules/sec
P_o	Source pressure
R	Radial distance from center of the target to the detector
T_g	Temperature of the gas
T_o	Stagnation temperature of the molecular beam source
T_s	Temperature of the solid
X	$2.3\ \epsilon/T$
α	Angle defined in Fig. 17
β	Angle defined in Fig. 17
ϵ	Lennard-Jones well-depth parameter
θ	Angle of reflection measured from the surface normal
$\Delta\theta$	$\theta_{spec} - \theta_{r_{max}}$
θ_i	Incident angle with respect to the surface normal of the molecular beam upon the target
$\theta_{r_{max}}$	Angle of maximum reflected intensity
θ_{spec}	Angle of specular reflection
ϕ	Angle defined in Fig. 16

SECTION I
INTRODUCTION

The atomic and molecular processes occurring at the gas-solid interface have been carefully studied both theoretically and experimentally during the past decade because of their importance in a variety of scientific and technical fields. The fields of rarefied gas dynamics, vacuum technology, and space simulation require a fundamental knowledge of gas-surface interaction phenomena.

The current theoretical models for the interaction of gases with solid surfaces are based on classical and quantum mechanics. The latter is the more general point of view, and the question is whether it is necessary from practical considerations to go to this level of complexity. Unfortunately, the modern quantum theories are not yet able to describe a wide range of gas and surface conditions. The majority of recent theoretical studies has been based on classical mechanics. Classical models which have successfully predicted energy accommodation and spatial distribution patterns for a variety of gas-surface combinations and conditions have been proposed by several authors (Refs. 1 through 5). Nevertheless, a completely satisfactory general theory of gas-surface interactions has yet to be established.

Most of the recent experimental work has been done with high temperature, single crystal surfaces and small gas-to-surface mass ratios (Refs. 6 and 7), and it is for these conditions that many of the contemporary theoretical models apply. However, a somewhat different and perhaps more fundamental experimental approach has been taken at AEDC. The interaction of a rare gas with its own crystalline phase has been studied under steady-state conditions. This approach offers two distinct advantages over previous experimental approaches:

1. The interaction potential parameters (e. g., the well-depth and range parameters for Morse and Lennard-Jones potentials) for argon-argon interactions are known.
2. The argon surface is clean because of continuous deposition by the incident beam. However, in the AEDC experiments the orientation and crystallographic structure of the surface are unknown.

SECTION II
EXPERIMENTAL APPARATUS

2.1 AERODYNAMIC MOLECULAR BEAM CHAMBER

The AEDC Aerodynamic Molecular Beam Chamber (Fig. 1, Appendix I) is a stainless steel cylinder, 3 ft in diameter by 6-1/2 ft long, which is divided into three sections (i. e., nozzle, collimation, and test) by two removable bulkheads. Vacuum conditions are produced and maintained in the cell by oil diffusion pumps, 20°K gaseous-helium (GHe)-cooled cryoliners, and 77°K liquid-nitrogen (LN_2)-cooled cryoliners. The total pumping speed for air is in excess of 500,000 liters/sec.

This system is capable of producing a 4-mm-diam beam with a variable flux from 2.0×10^{13} to 4.0×10^{16} molecules/sec while maintaining a background pressure of 3.0×10^{-8} torr in the test section. During the experimental runs, the operating pressures were 4×10^{-4}, 2×10^{-7}, and 3×10^{-8} torr in the nozzle, collimating, and test sections of the chamber, respectively. A complete description of the beam system and its performance is given in Ref. 8.

2.2 HIGH TEMPERATURE AERODYNAMIC BEAM SOURCE

The high temperature beam source is a resistance-heated tantalum tube 4 in. in length with 0.25-in. outside diameter and 0.02-in. wall thickness (Fig. 2). A 0.014-in.-diam hole is drilled through the wall at a position halfway between the ends of the tube. The beam gas enters through both ends and is expanded through the small orifice. Electrical power is supplied by copper electrodes attached near the tube ends. A water-cooled copper heat shield is placed around the tantalum source to protect the cryopanels from the radiating heat load.

2.3 TARGET SUBSTRATE

The target substrate for these experiments is a hand-polished copper disk. The disk is hollow so that GHe can be circulated through it. The substrate temperatures in the range from 30 to 15°K are measured by a hydrogen vapor pressure thermometer and in the range of from 68 to 30°K by Chromel®-constantan thermocouples.

2.4 DETECTION SYSTEMS

One of the major problems in molecular beam experiments is to extract the signal caused by the reflected beam molecules from the background noise. The 3.0×10^{-8} torr background pressure during these experiments is equivalent to 10^{12} molecules/sec-cm^2 striking the detector. The molecular intensity reflected from the target surface, however, is also on the order of 10^{12} molecules/sec-cm^2. Therefore, it is necessary that the detection system be able to distinguish the beam signal from a background noise level of equal intensity. To accomplish this, a modulated beam system is used, which consists of (1) a mechanical chopper, (2) a quadrupole mass spectrometer, and (3) a lock-in amplifier (Figs. 3 and 4). This detection system has the capability of recovering beam intensity signals that are three orders of magnitude less than the background gas intensity. A complete description of the detector and its performance is given in Ref. 9.

The total beam flux is measured by using a miniature ionization gage. The gage is enclosed in the standard glass envelope, but the normal 1-in.-diam opening was reduced to 6 mm in order to increase the directional sensitivity (Fig. 5).

2.5 TARGET AND DETECTOR MOVEMENT MECHANISMS

The target and detector are rotated by chain drives that are manually controlled through mechanical feedthroughs in the test section of the chamber. The target and detector can be positioned with an accuracy of ±2 deg.

SECTION III
EXPERIMENTAL TECHNIQUE AND PROCEDURES

The first steps in studying particle-surface interactions are to evaluate the basic parameters relating to the incident molecules and to define the surface conditions, if possible. In this series of tests, an aerodynamic molecular beam was used to provide the incident molecules. Therefore, the objective of the first experiments was to define the beam characteristics.

3.1 CHARACTERISTICS OF THE BEAM

Aerodynamic beams differ from the classical oven beams in several areas: (1) the intensity is greater, (2) the mean energy is higher, (3) the molecules in the beam can exist as single atoms or the beam molecules may form polymers held together by van der Waals forces (Ref. 10), and (4) the velocity distribution is very narrow. For instance, at Mach 20, the velocity distribution of an aerodynamic beam is such that 80 percent of the beam molecules have a velocity that is within 5 percent of the mean velocity (Ref. 11).

3.1.1 Total Beam Flux and Polymerization in the Beam

A detailed description of the beam components and an analysis of the free jet expansion are given in Ref. 12, and typical beam performance data are shown in Fig. 6.

The data in Fig. 6 were obtained by lowering the miniature ionization gage into the beam and obtaining the gage reading as the source pressure was varied over the desired range.

The source pressure, P_o, was varied by adjusting a needle valve in the source gas supply line. Previous calibration with an oven beam source has shown that if the ionization pressure gage reading for argon is multiplied by 2.5×10^{20} the product is the total beam flux in molecules per second.

The curves in Fig. 6 indicate the change in the total beam flux as the temperature varies from 1700 to 2500°K. The drop in the beam flux at the higher source pressures is caused by polymerization in the beam and skimmer interaction. Experimental data relating to the onset of polymerization in argon beams with high source pressures are presented in Ref. 10, and skimmer interactions are discussed in Ref. 13.

Partial pressure measurements taken at source pressures from 1000 to 3000 torr show that detectable amounts of polymerization begin to occur at the peak in the curve and increase rapidly with increasing source pressure. The source pressure was maintained low enough to ensure that polymerization would not occur during these experiments. Therefore, the data to be presented in this investigation are only for argon atoms.

3.1.2 Intensity Cross Section of the Beam

Measurements were made with an ionization gage to determine the intensity (molecules/sec-cm^2) at various points across the beam. A

plate with a 0.014-in.-diam hole was placed over the ionization gage opening. Readings were then taken at positions visually measured with a transit. The beam intensity distribution has a uniform core as shown in Fig. 7.

3.2 SURFACE PREPARATION

During these experiments, the solid argon target surface was prepared by the partial capture of the impinging argon molecular beam on the cryogenically cooled copper substrate. The surfaces were deposited by beams having various angles of incidence and at both constant and continuously decreasing substrate temperatures. The incident strike rates were 3.25×10^{15} and 1.1×10^{16} molecules/sec-cm^2. The experimental data were not affected by any of these surface preparation conditions. The argon cryodeposits appeared to be crystalline or glassy but the uniformity or orientation of the crystallographic structure is unknown. Because of the difficulties associated with growing large crystals of argon (Ref. 14), the cryodeposit is probably polycrystalline argon. Thus, during these experiments, the solid argon target surface is continuously deposited and therefore "clean" but undefined in terms of macroscopic crystal structure.

3.3 EXPERIMENTAL PROCEDURE

To measure the signal from the reflected argon atoms, an arrangement as shown in Fig. 3 was used. The target could be rotated to change the angle of incidence. To change the angle at which the reflected signal was being measured, the detector could be moved in an arc about the target. When the detector was maintained in the plane defined by the incident beam and the normal to the target surface, the measurements made are called "in-plane" measurements. Also, a limited number of "out-of-plane" measurements were made by moving the detector along its arc track (Fig. 3).

The specific experimental procedures were as follows: The beam source temperature and pressure were adjusted to the desired values, and the target was positioned to provide the desired angle of incidence. The target was cooled to 36°K and the spatial distribution of the reflected beam molecules was determined. These data provided a reference for the performance of the detector system as argon does not condense on a 36°K surface and previous experiments have shown that the spatial distribution of the reflected beam molecules was cosine.

The target was then cooled to 15°K. However, at a target temperature of approximately 30°K the beam molecules began to condense. This phenomenon was not investigated in detail but the data indicated that at first the capture coefficient was near unity. Then as the cryodeposit thickness increased to a few microns the capture coefficient decreased and finally a steady-state value was measured. The data reported in this report were obtained after the capture coefficient had reached a steady-state value.

Spatial distribution data for the molecules departing from the surface were taken as the detector was moved through increments of 2, 5, or 10 deg. (The angles were measured with respect to the surface normal.) However, because of the beam width and the size of the detector, data could not be taken within 20 deg of the beam.

SECTION IV
EXPERIMENTAL RESULTS AND DISCUSSION

4.1 SPATIAL DISTRIBUTIONS OF HIGH TEMPERATURE ARGON BEAMS

4.1.1 Introduction

The spatial distribution data (Figs. 8 through 16) are presented as polar coordinate graphs to give a more realistic picture of the reflection patterns. The distance along a ray is directly proportional to the signal strength. Also, it should be noted that both the incident and reflected angles are measured with respect to the surface normal.

4.1.2 In-Plane Measurements

The experimental data shown in Fig. 8 indicate that diffuse scattering, i. e., cosine reflection (T_o = 2500°K), occurs for 0.54-ev argon striking a 36°K copper target at an incident angle of 60 deg. Under these experimental conditions, argon does not condense on a 36°K surface. Nevertheless, the surface is contaminated to an unknown degree by condensation of residual gases such as water vapor (H_2O) (Ref. 15). These data provide a check on the performance of the detector systems as previous experiments have shown that the spatial distribution of the reflected beam molecules is cosine (Ref. 12). When the temperature of the copper substrate was lowered to 30°K, condensation of the gaseous argon began on the surface, and a visible argon cryodeposit formed on the copper target. After several minutes, the number of reflected argon atoms reached a steady-state value, and spatial distribution data for the argon molecules leaving the surface was obtained.

The effect of argon beam energy for an incident angle of 60 deg impinging on a 15°K argon cryodeposit is shown in Fig. 9. Supraspecular spatial distributions were observed for beams in the temperature range from 1400 to 2500°K. The angle of maximum reflected intensity in the forward lobes was independent of the beam energy and was observed to be 78 ± 2 deg. As the source gas temperature increases, the capture of the incident beam decreases. Estimates of the capture coefficient are presented in Appendix II.

For small angles of incidence and a beam energy of 0.54 ev, argon gas atoms are reflected in both the forward and backward directions from the argon cryosurface as shown in Figs. 10 and 11. The magnitude of the backward flux is a strong function of the angle of incidence and increased as θ_i approached 0. The angle of maximum reflected intensity in the forward lobes was once again 78 ± 2 deg, indicating that this angle is also independent of the angle of incidence.

Since the sublimation energy of solid argon (0.08 ev) is considerably less than the mean energy of the beam used in these experiments, sputtering[1] of the argon cryodeposit is possible. However, when an argon beam at various angles of incidence (Fig. 12) and at various energies (Fig. 13) was directed on a carbon dioxide cryodeposit (sublimation energy ≈ 0.306 ev, Ref. 15) sputtering was not observed. Also, a nitrogen cryodeposit (sublimation energy ≈ 0.06 ev) was not observed to be sputtered by a 0.54-ev argon beam. Nevertheless, sputtering is still possible, and a more definitive experiment is being planned.

4.1.3 Out-of-Plane Measurements

Out-of-plane measurements of the spatial flux distribution of a 0.54-ev argon beam at incident angles of 60 and 5 deg are shown in Figs. 14 and 15. The geometry for these experiments is shown in Fig. 16 for an out-of-plane angle, ϕ, of 45 deg. As in the in-plane case, the angle of maximum reflected intensity is independent of the angle of incidence and occurs at 78 ± 2 deg. For the estimation of the capture coefficient (Appendix II) for 60-deg angle of incidence, symmetry about the ray corresponding to the maximum detector signal was assumed. This is supported by the fact that for a 0.54-ev argon beam at θ_i = 60 deg, the detector signal for the out-of-plane measurements was less than the corresponding in-plane signals and approximately equal to the value predicted by the assumption of symmetry.

---

[1]Sputtering as used in this report refers to the ejection of surface atoms by the excess energy of the impinging beam atoms.

4.2 CAPTURE COEFFICIENT

Using the technique described in Appendix II, it was determined that the capture coefficient of a 15°K argon frost for a 2500°K argon beam with normal incidence was 0.99 ± 0.01. The implications of these data are not evident until the energies involved are considered. The mean energy of the incident beam is 0.54 ev (i. e., T_o = 2500°K) and the sublimation energy of solid argon is approximately 0.08 ev. Therefore, when a 0.54-ev argon atom strikes a surface and condenses, the amount of energy transferred to the surface is equivalent to the amount required to evaporate six surface atoms. However, these data have shown that a 0.54-ev argon atom will condense on a 15°K surface and that the total reflected, evaporated, and sputtered molecular flux departing the surface is less than 1 percent of the incident beam flux. Thus any theoretical model that adequately describes the hot gas-cold surface interaction process for argon must allow for the rapid transfer of energy from the colliding atom to the surface. This implies that several surface atoms must be included in the argon-argon model and perhaps in a rigorous model of the general particle-surface interaction processes.

Other parameters of prime importance in previous treatments of particle-surface interaction are the angle of incidence and the energy of the incident atoms (Ref. 16). These present studies show that these same parameters are of prime importance during an argon-argon particle-surface interaction. The capture coefficient is a strong function of incident beam energy (i. e., source temperature) and the angle of incidence. However, it should be stated that calculation of the capture coefficient for angles of incidence less than 90 deg as outlined in Appendix II is not rigorous but the predicted trends are valid.

4.3 DISCUSSION OF THE APPLICATION OF CONTEMPORARY THEORETICAL MODELS TO THE EXPERIMENTAL DATA

The AEDC experimental data of the spatial distributions of argon gas-argon solid collisions are unique in that the mass ratio is unity and the surface is at cryogenic temperatures. As stated in Section I, most experimental and theoretical work has been done with high temperature, single crystal surfaces and small gas-to-surface mass ratios. For example, Stickney's "hard cube" model (Ref. 1) which has successfully predicted lobular spatial distributions for a variety of gas and surface conditions only applies for mass ratios of one-third or less and thus is not applicable to the present results. Trilling's model (Ref. 2) also depends upon the assumption that the ratio of the masses of the gas and

surface atoms is small. On the other hand, Goodman's n-D lattice model (Ref. 3) would perhaps be applicable if modified for unity mass ratio. Also, his assumption that the thermal motion of the surface atoms can be neglected (i. e., the temperature of the solid is at 0°K) would be more justifiable since for the argon-argon interactions the solid was maintained at 15°K.

Hurlbut, using analog computation, studied the interaction of argon on condensed argon by means of a simple cubic, two-dimensional, nonlinear lattice model. Although his complete results have not been published, Hurlbut found that for 1.04-ev argon incident at 60 deg on solid argon, the angle of maximum reflected intensity was approximately 70 deg (Ref. 4).

Oman's computer model (Ref. 5) for the three-dimensional interactions of gas molecules with an ideal surface perhaps offers another suitable theoretical approach if modified for a mass ratio of unity. Unfortunately, the models of Goodman, Hurlbut, and Oman require extensive electronic computation, and thus a direct comparison of the present data with these theories is not attempted.

The experimental data for argon-argon collisions do exhibit some of the general characteristics for scattering patterns as presented by Stickney in his review (Ref. 16):

1. $\frac{\partial(\Delta\theta)}{\partial T_g} \leq 0$

2. $\frac{\partial(\Delta\theta)}{\partial T_s} \geq 0$

3. $\frac{\partial\theta_{r_{max}}}{\partial\theta_i} \geq 0$

4. $\frac{\partial(\Delta\theta)}{\partial Mg} > 0$ when $\Delta\theta > 0$, $\frac{\partial(\Delta\theta)}{\partial Mg} < 0$ when $\Delta\theta < 0$

5. The dispersion of the scattering patterns increases with m_g

6. Supraspecular patterns are most likely to occur when both $T_g > T_S$ and $\theta_i << 90$ deg

7. Nondiffuse scattering is most likely to occur from target surfaces that are smooth and free of gross contamination

8. The dispersion of nondiffuse scattering is greater for the in-plane pattern than for the out-of-plane pattern.

As shown in Fig. 17a, the data have characteristic (1) since $\Delta\theta$ remains constant as the gas temperature increases, i. e., $(\partial\Delta\theta/\partial T_g) = 0$. In the AEDC experiments the surface temperature was constant, and thus characteristic (2) cannot be checked. Figure 17b shows that for various angles of incidence $\theta_{r_{max}}$ remains constant, i. e., $(\partial\theta_{r_{max}}/\partial\theta_i) = 0$, and thus the data have characteristic (3). The first condition of characteristic (6) was applicable since supraspecular scattering patterns were observed for $T_g > T_s$. However, the second condition, i. e., $\theta_i << 90$ deg, was not applicable since supraspecular scattering was observed for $\theta_i = 90$ deg.

SECTION V
SUMMARY AND CONCLUSIONS

The results of a preliminary investigation of the spatial distribution of argon reflected from its own solid have been presented. The supraspecular flux distributions were highly lobular for all angles of incidence when solid argon was used as the target surface. It was observed that the angle of maximum reflected intensity was independent of both beam incident angle and beam energy. For angles less than 5 deg of incidence, backward lobes were observed. The capture coefficient was a function of both incident beam energy and beam angle of incidence. For small angles of incidence and a beam temperature of 2500°K, the capture coefficient was near unity but decreased with increasing incident angle to an estimated value of approximately 0.5 at a 60-deg incident angle.

There have apparently been no previous experimental studies of the spatial distribution of a rare gas reflected from its own solid. Lobular distributions similar to those in Fig. 9 have been reported for the scattering of inert gases from various metal surfaces (Ref. 16), but there have been no distributions reported similar to those shown in Figs. 10 and 11 for nearly normal incidence.

The current theoretical models which have been published either do not apply or must be modified in order to comply with the experimental conditions. Future attempts to explain these data will be aided by the fact that the interaction parameters for argon-argon collisions are known (Ref. 17).

REFERENCES

1. Stickney, R. E. and Logan, R. M. "Simple Classical Model for the Scattering of Gas Atoms from a Solid Surface." J. Chem. Phys., Vol. 44, No. 1, 1966, p. 195.
2. Trilling, L. "A Theory of Accommodation." J. de Mechanique, Vol. 3, No. 2, 1964, p. 215.
3. Goodman, F. O. "On the Theory of Accommodation Coefficients III. Classical Perturbation Theory for the Thermal Accommodation of Light Gases." RAE Technical Note CPM 17, May 1963.
4. Hurlbut, F. C. "Current Developments in the Study of Gas-Surface Interactions." Fifth Rarefied Gas Dynamics Symposium. C. L. Brundin, ed., Vol. 1, Academic Press, New York, 1967, pp. 1-34.
5. Oman, R. A., Bogan, A., and Li, C. H. "Theoretical Prediction of Momentum and Energy Accommodation for Hypervelocity Gas Particles on an Ideal Crystal Surface." Grumman Research Department Report RE-111J, 1964.
6. Smith, J. N., Jr. and Saltsburg, H. "Recent Studies of Molecular Beam Scattering from Continuously Deposited Gold Films." Proceedings of the Fourth International Symposium on Rarefied Gas Dynamics. J. H. de Leeuw, ed., Vol. II, Academic Press, New York, 1966, pp. 491-504.
7. O'Keefe, D. R. "The Scattering of High Energy Argon Atoms from a Well Characterized (100) Tungsten Surface." UTIAS Report No. 132, July 1968.
8. Brown, R. F. and Heald, J. H., Jr. "Description and Performance of a Molecular Beam Chamber Used for Cryopumping and Adsorption Pumping Studies." AEDC-TR-66-135 (AD641388), October 1966.
9. Heald, J. H., Jr. "Performance of a Mass Spectrometric Modulated Beam Detector for Gas-Surface Interaction Measurements." AEDC-TR-67-35 (AD648984), March 1967.
10. Brown, R. F. and Busby, M. R. "Molecular Beam Studies of Polymerization and Condensation in Free-Jet Expansions of Argon and Nitric Oxide." AEDC-TR-68-245 (AD843325), November 1968.
11. Anderson, J. B., Andres, R. P., and Fenn, J. B. "Supersonic Nozzle Beams." Advances in Chemical Physics, J. Ross, ed., Vol. X, John Wiley and Sons, Inc., New York, 1966, pp. 275-318.

12. Caldwell, R. C., Busby, M. R., and Brown, R. F. "Spatial Distributions of 285°K to 2500°K Argon Beams Scattered from an Undefined Copper Surface at Low Temperatures." AEDC-TR-69-142, to be published.

13. Brown, R. F. and Heald, J. H., Jr. "Background Gas Scattering and Skimmer Interaction Studies Using a Cryogenically Pumped Molecular Beam Generator." Fifth Rarefied Gas Dynamics Symposium. C. L. Brundin, ed., Vol. 2, Academic Press, New York, 1967, p. 1407.

14. Peterson, O. G., Batchelder, D. N., and Simmons, R. O. "X-Ray Diffraction Study of Argon Crystal Growth." Journal of Applied Physics, Vol. 36, No. 9, 1965, p. 2682.

15. Heald, J. H., Jr. and Brown, R. F. "Measurements of Condensation and Evaporation of Carbon Dioxide, Nitrogen, and Argon at Cryogenic Temperatures Using a Molecular Beam." AEDC-TR-68-110 (AD674596), September 1968.

16. Stickney, R. E. "Atomic and Molecular Scattering from Solid Surfaces." Advances in Atomic and Molecular Physics. D. R. Bates and I. Esterman, eds., Vol. 3, Academic Press, New York, 1967, pp. 143-204.

17. Hirschfelder, J. O., Curtiss, C. F., and Bird, R. B. Molecular Theory of Gases and Liquids. John Wiley and Sons, Inc., New York, 1954, p. 168.

18. Hinchen, J. J. and Shepherd, E. F. "Molecular Beam Scattering from Surfaces of Various Metals." Fifth Rarefied Gas Dynamics Symposium. C. L. Brundin, ed., Vol. 1, Academic Press, New York, 1967, p. 239.

19. Goodman, F. O. "Classical Perturbation Theory of the Thermal Accommodation Coefficient in n-Dimensions." Surface Science, Vol. 11, No. 2, 1968, p. 283.

APPENDIXES

I. ILLUSTRATIONS

II. AN ESTIMATION OF THE BEAM CAPTURE COEFFICIENT FOR ARGON GAS-ARGON CRYSTAL INTERACTIONS

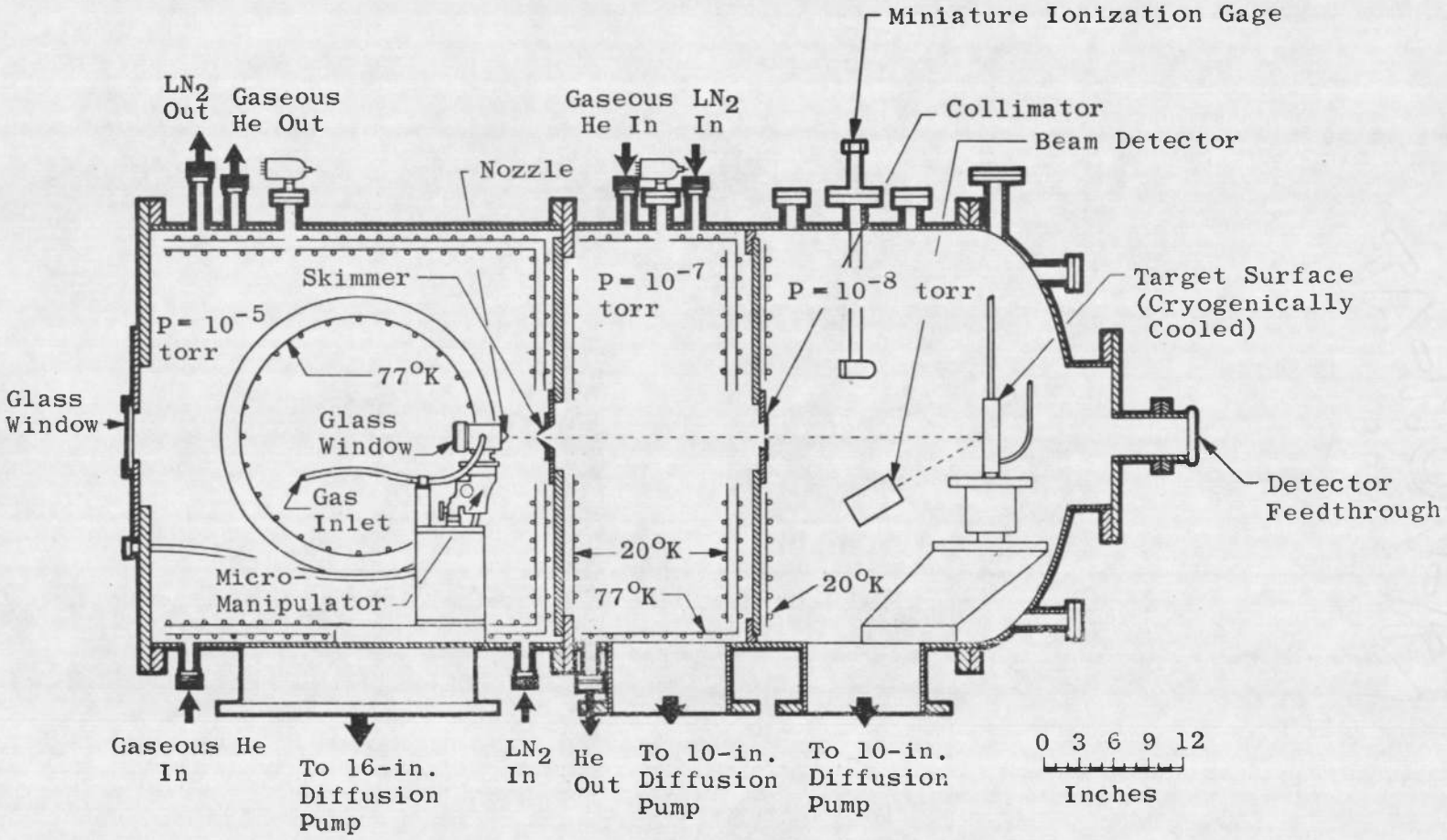

Fig. 1 Aerodynamic Molecular Beam Chamber

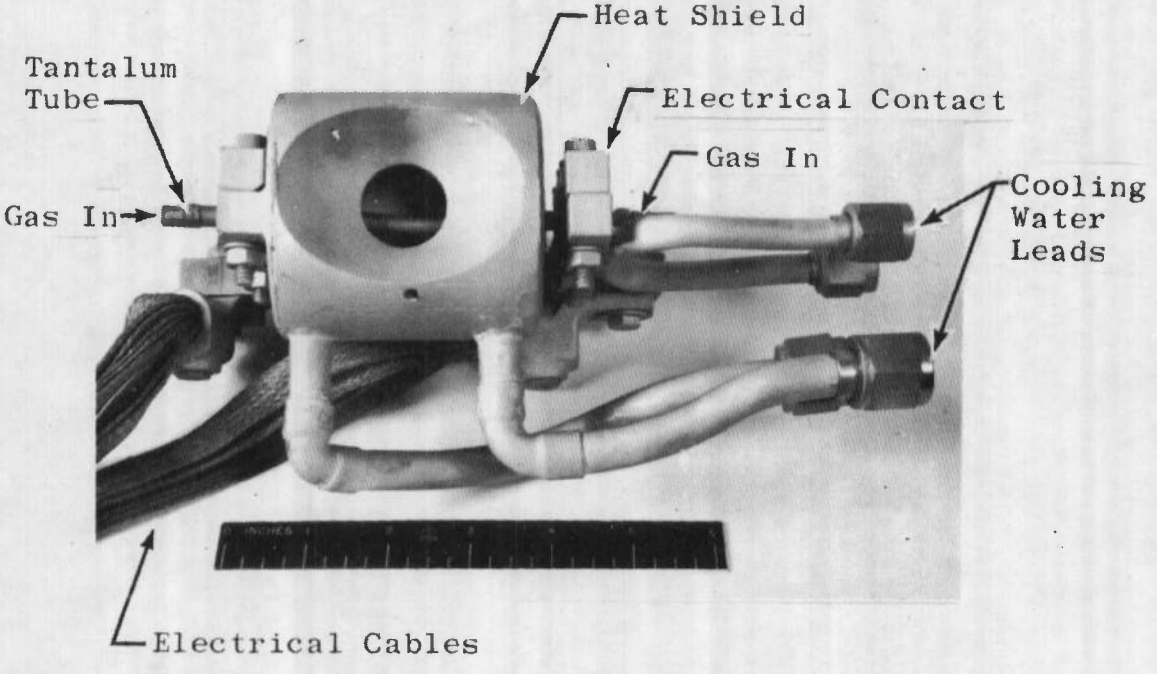

Fig. 2 Photograph of the High Temperature Beam Source

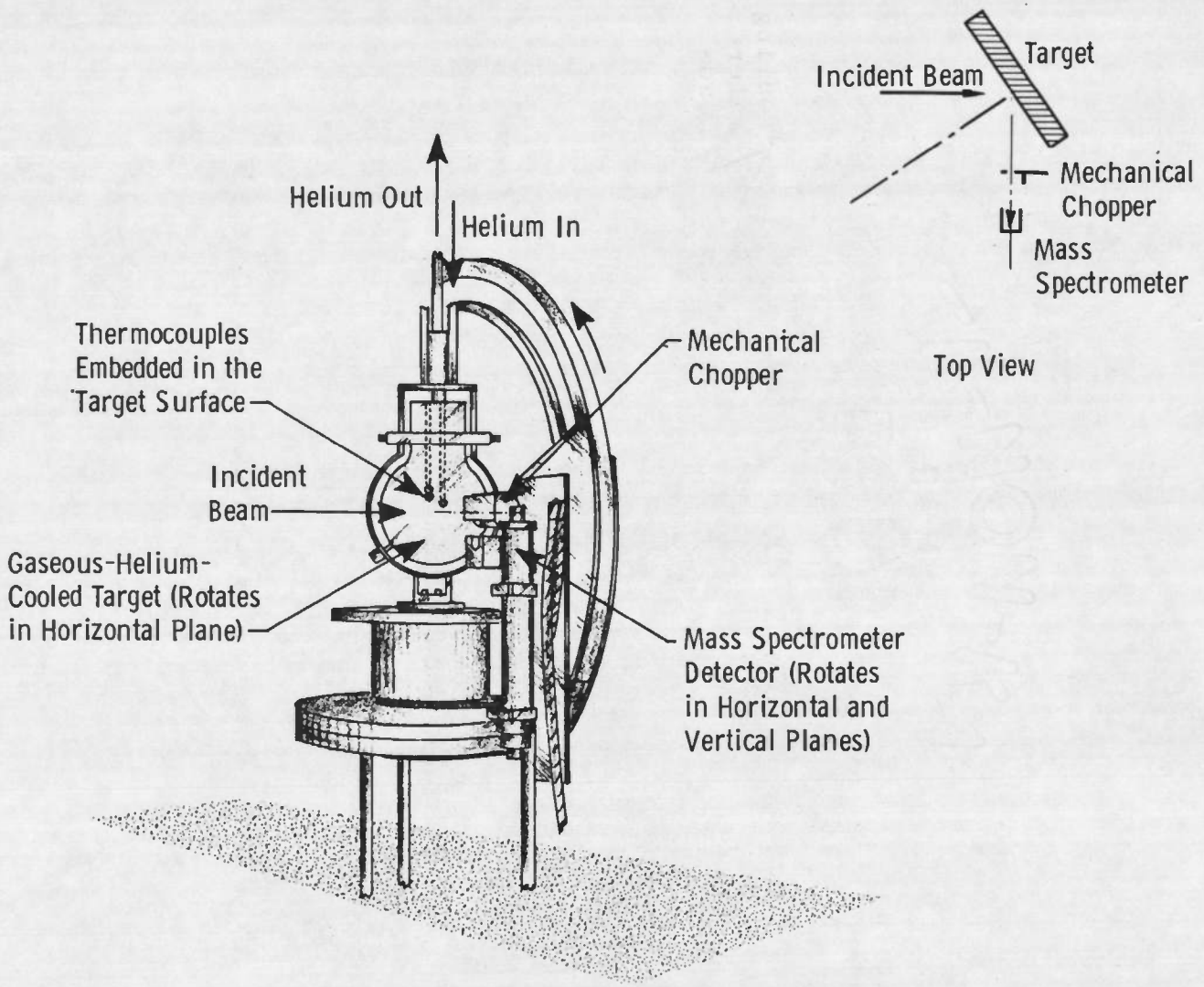

Fig. 3 Schematic of the Detection System Components

AEDC-TR-69-195

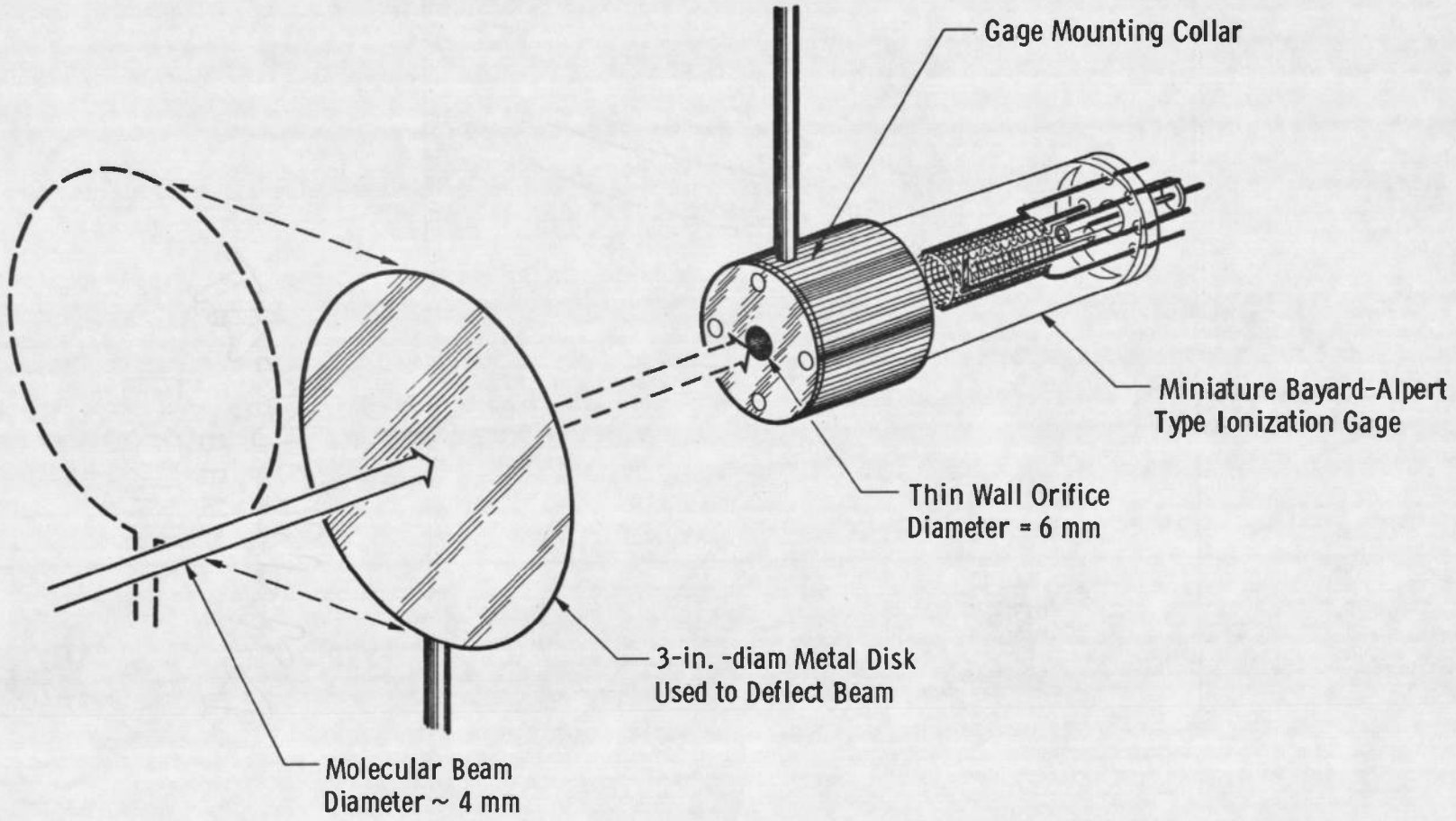

Fig. 5 Molecular Beam Detector

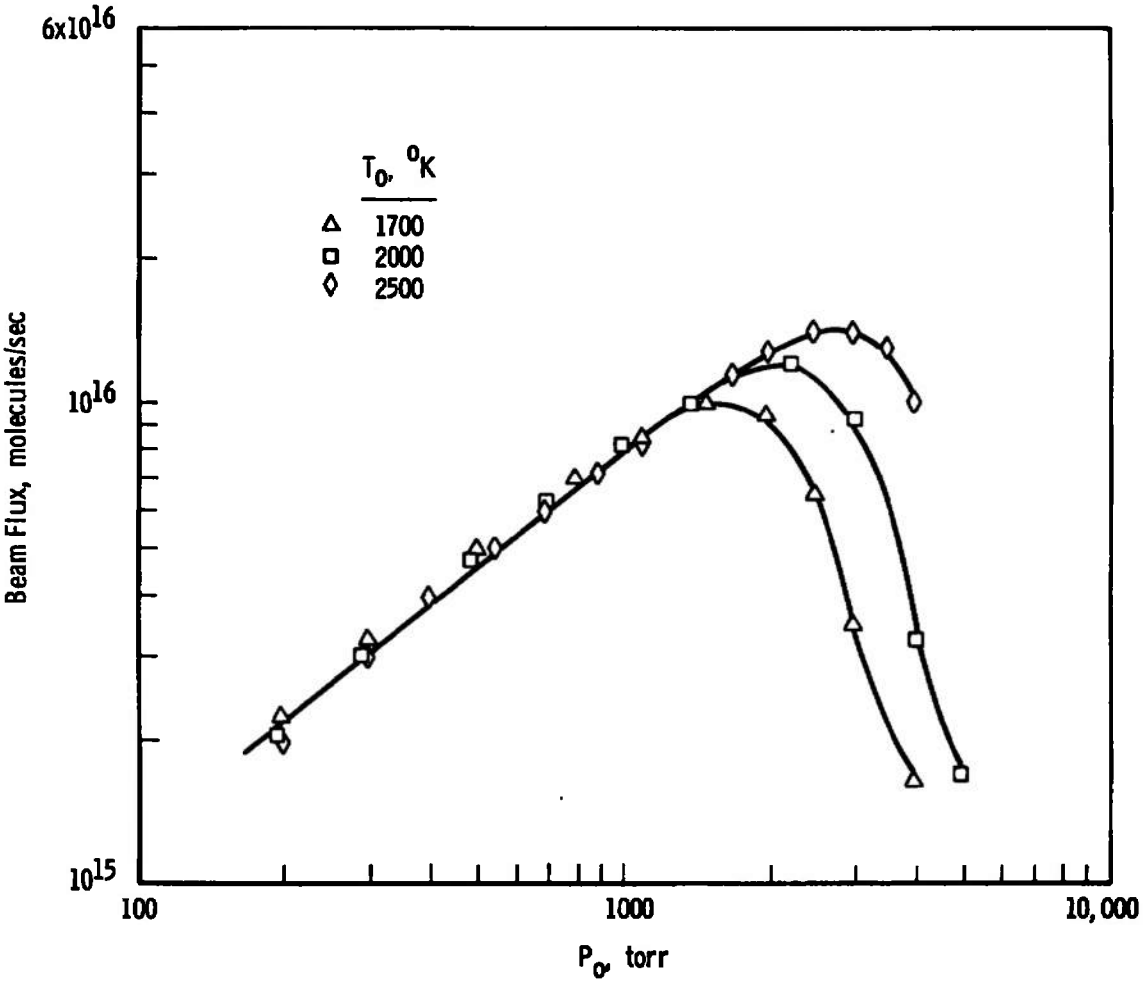

Fig. 6 Argon Beam Performance

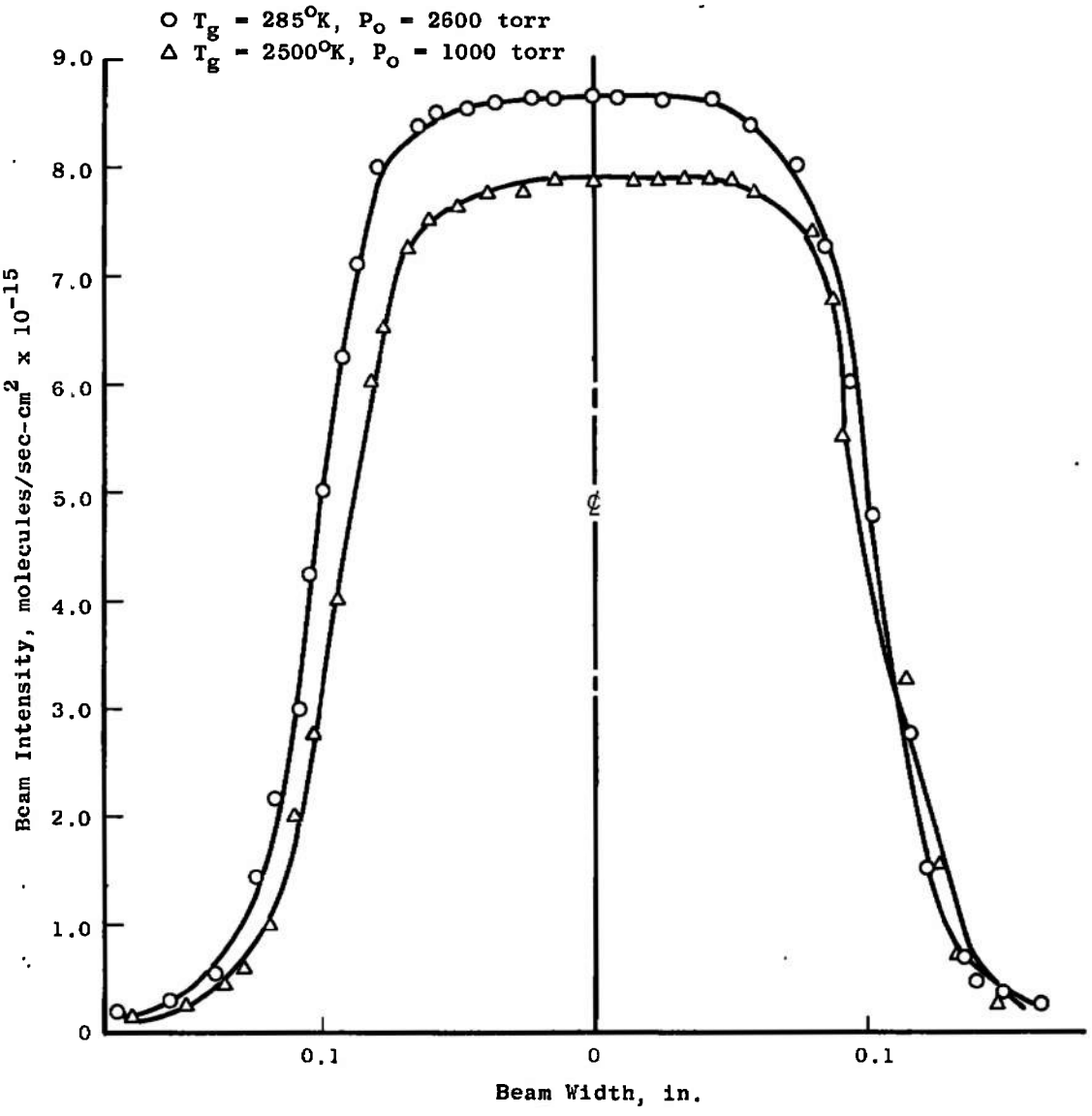

Fig. 7 Intensity Cross Section of the Beam

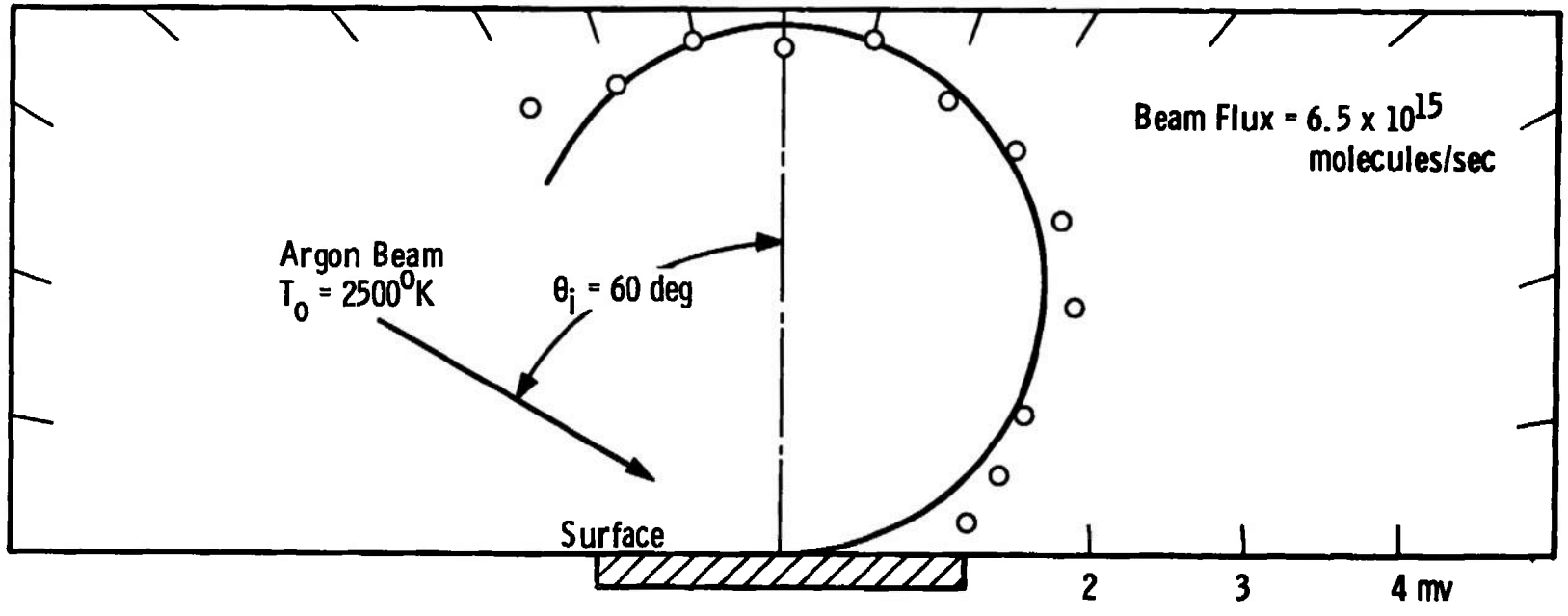

Fig. 8 Spatial Distribution of 2500°K Argon Reflected from a 36°K Copper Surface

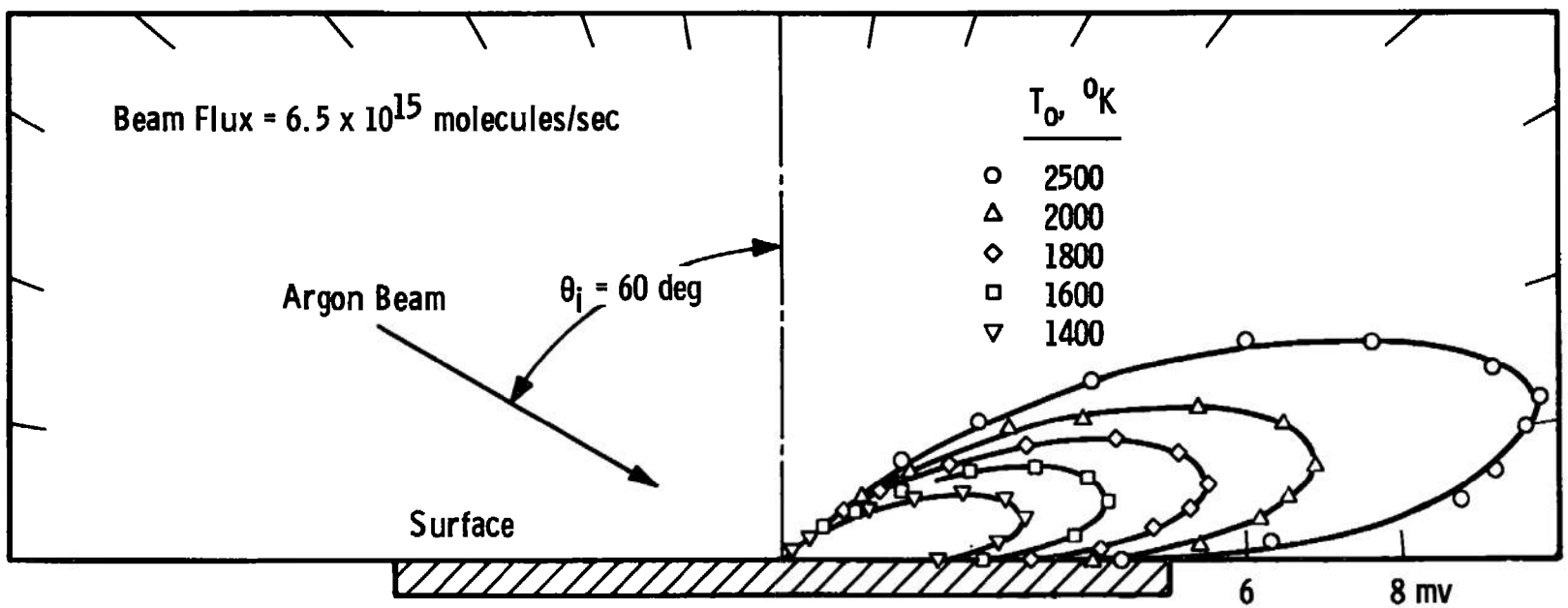

Fig. 9 Spatial Distribution of High Temperature Argon Reflected from a 15°K Cryosurface

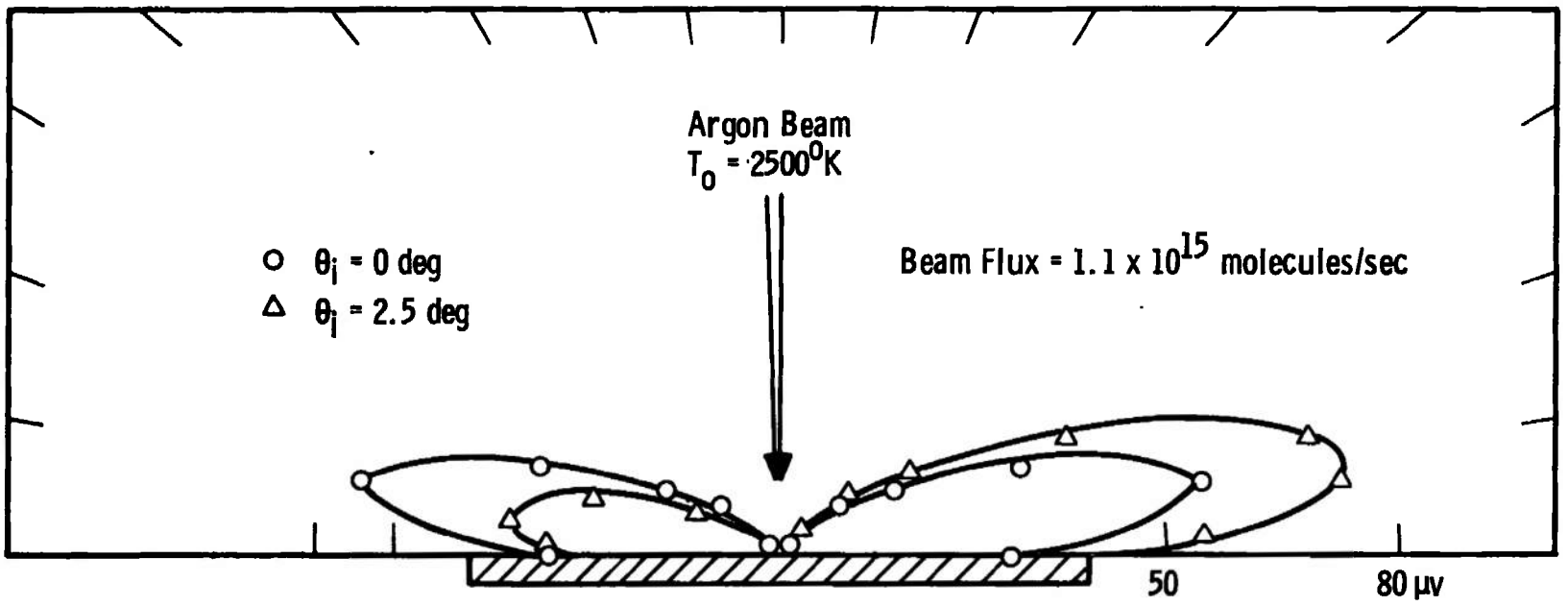

Fig. 10 Spatial Distribution of 2500°K Argon Reflected from a 15°K Cryosurface at Several Angles of Incidence

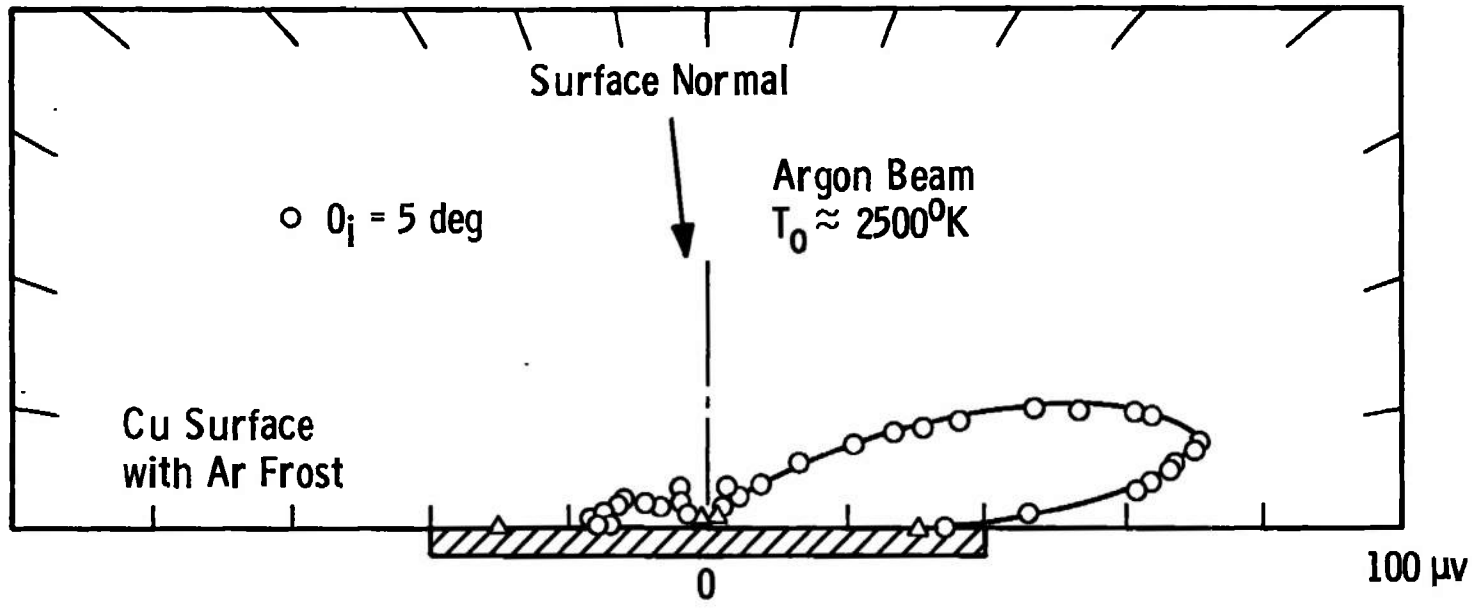

Fig. 11 Spatial Distribution of 2500°K Argon Reflected from a 15°K Cryosurface at 5-deg Angle of Incidence

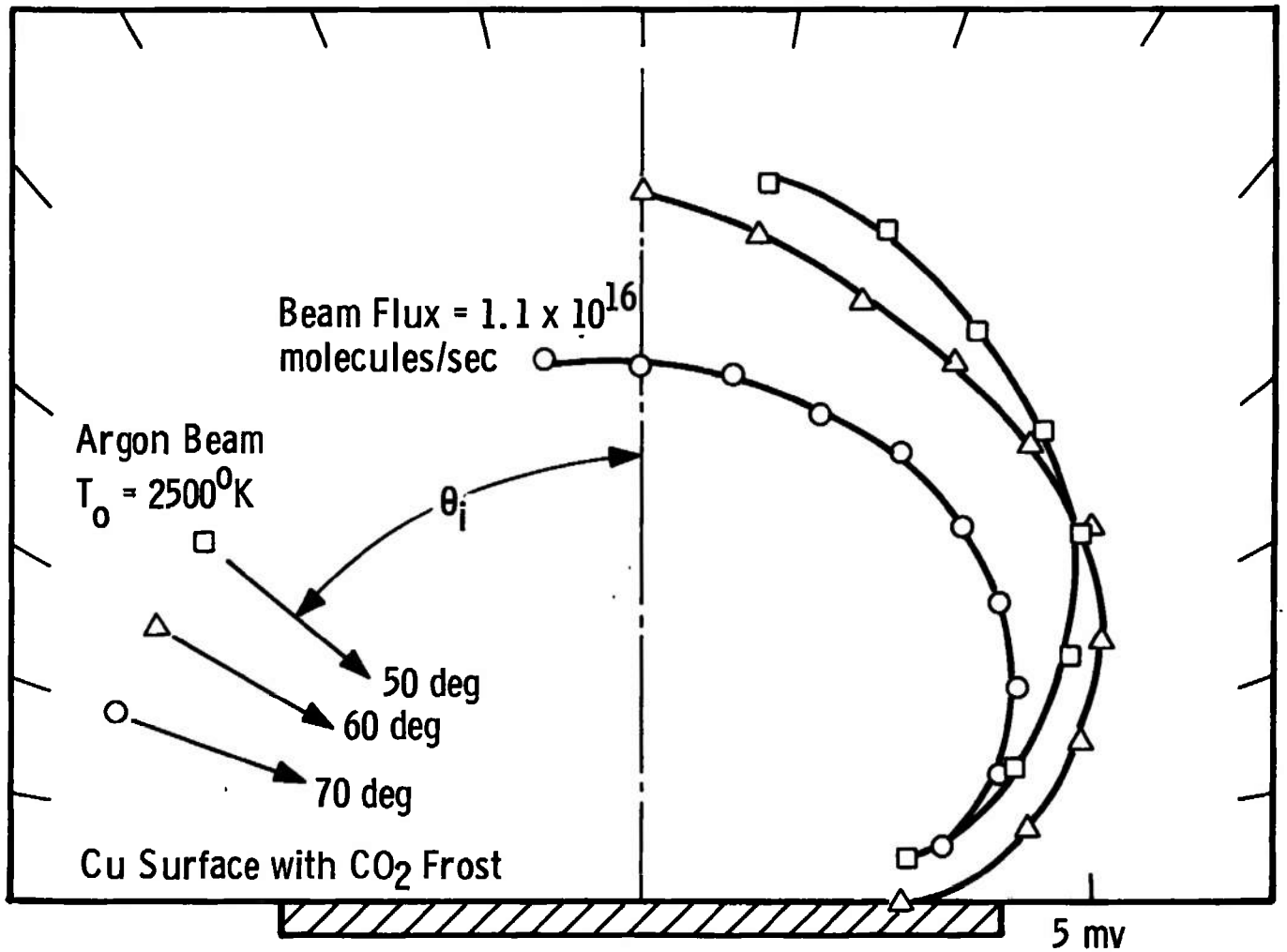

Fig. 12 Spatial Distribution of 2500°K Argon Reflected from a 68°K Carbon Dioxide Cryosurface for Various Incident Angles

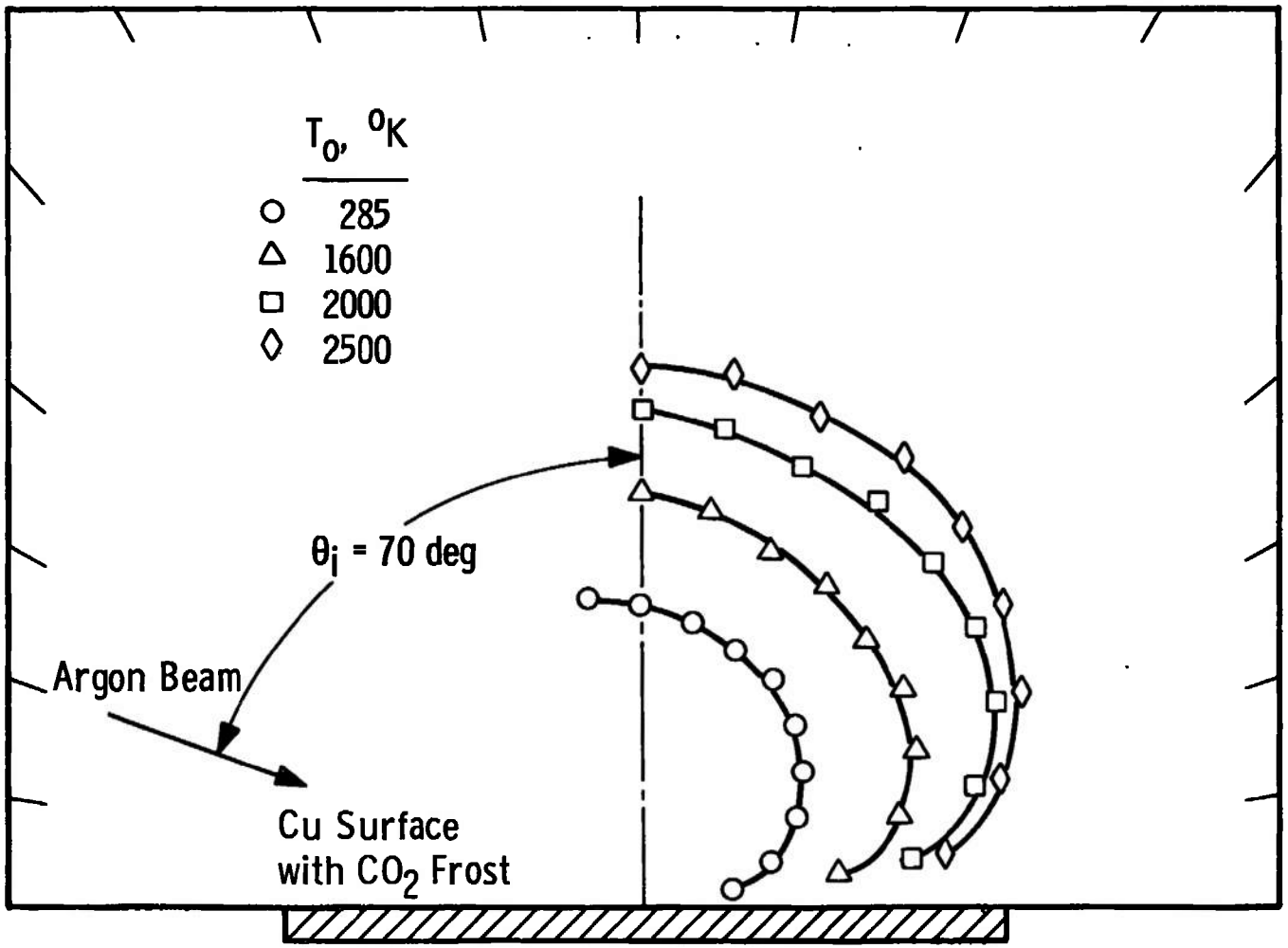

Fig. 13 Spatial Distribution of Argon Reflected from a 68°K Carbon Dioxide Cryosurface for Various Beam Temperatures

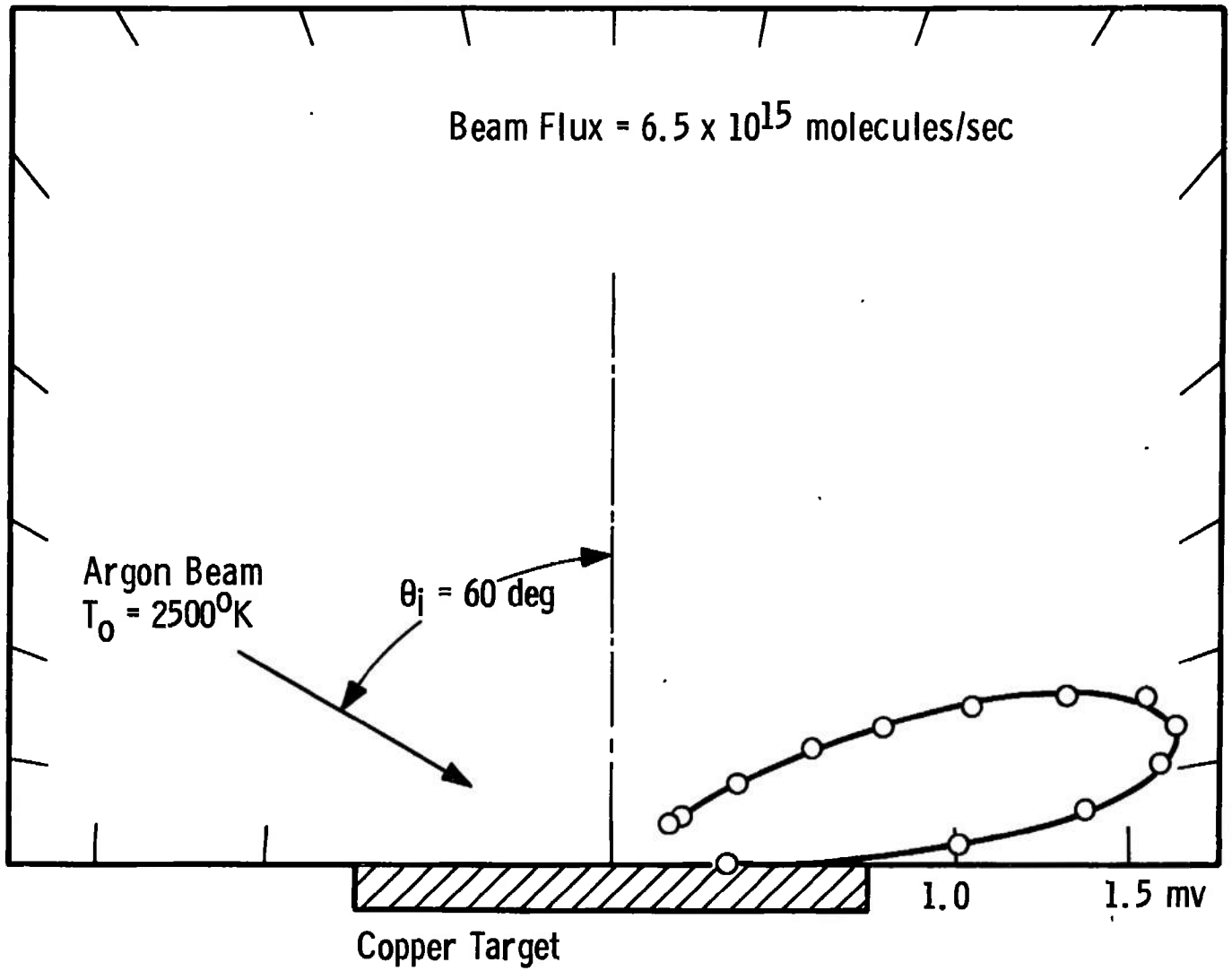

Fig. 14 Out-of-Plane (ϕ = 45 deg) Spatial Distribution of 2500°K Argon Reflected from a 15°K Cryosurface at 60-deg Angle of Incidence

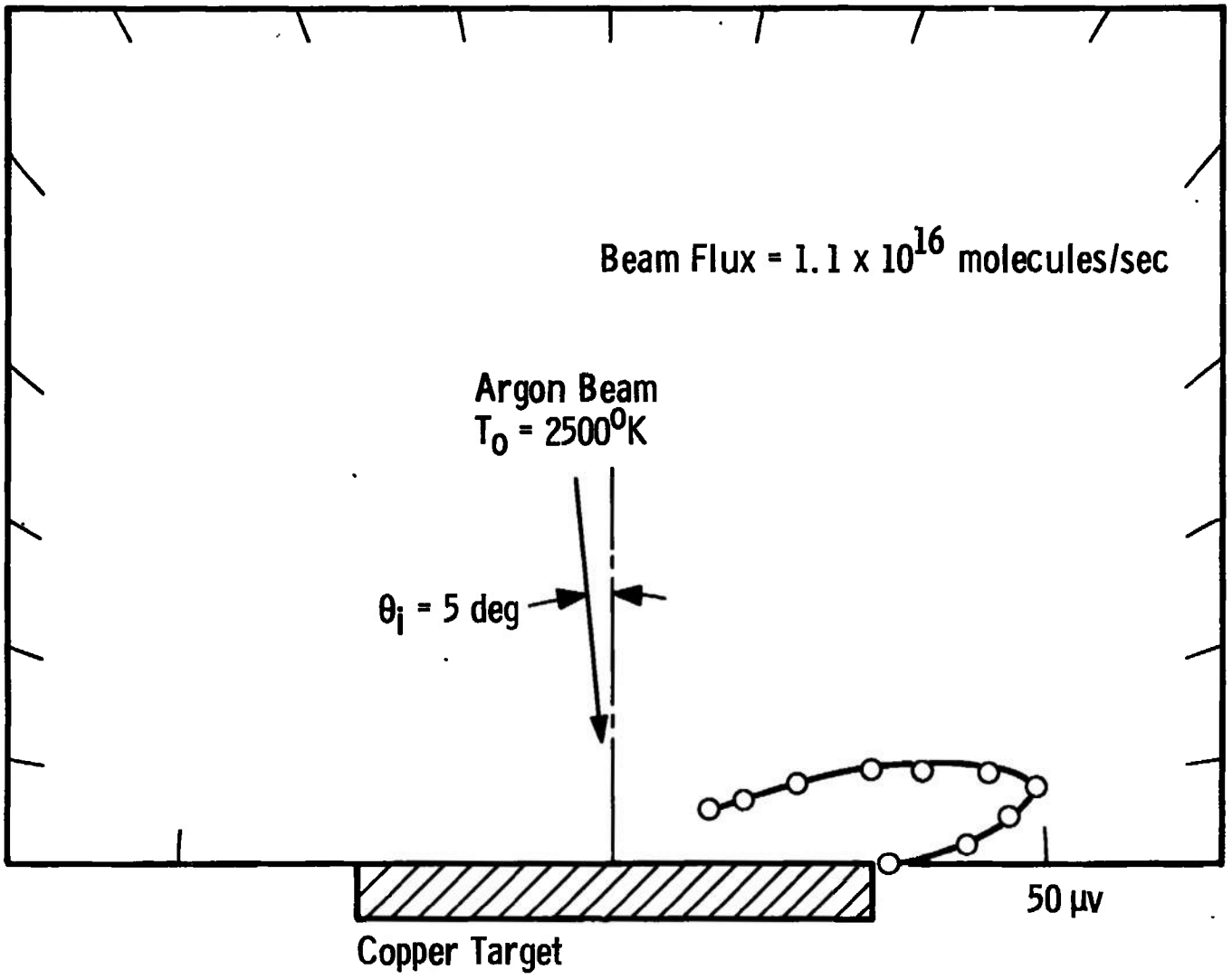

Fig. 15 Out-of-Plane (ϕ = 45 deg) Spatial Distribution of 2500°K Argon Reflected from a 15°K Cryosurface at 5-deg Angle of Incidence

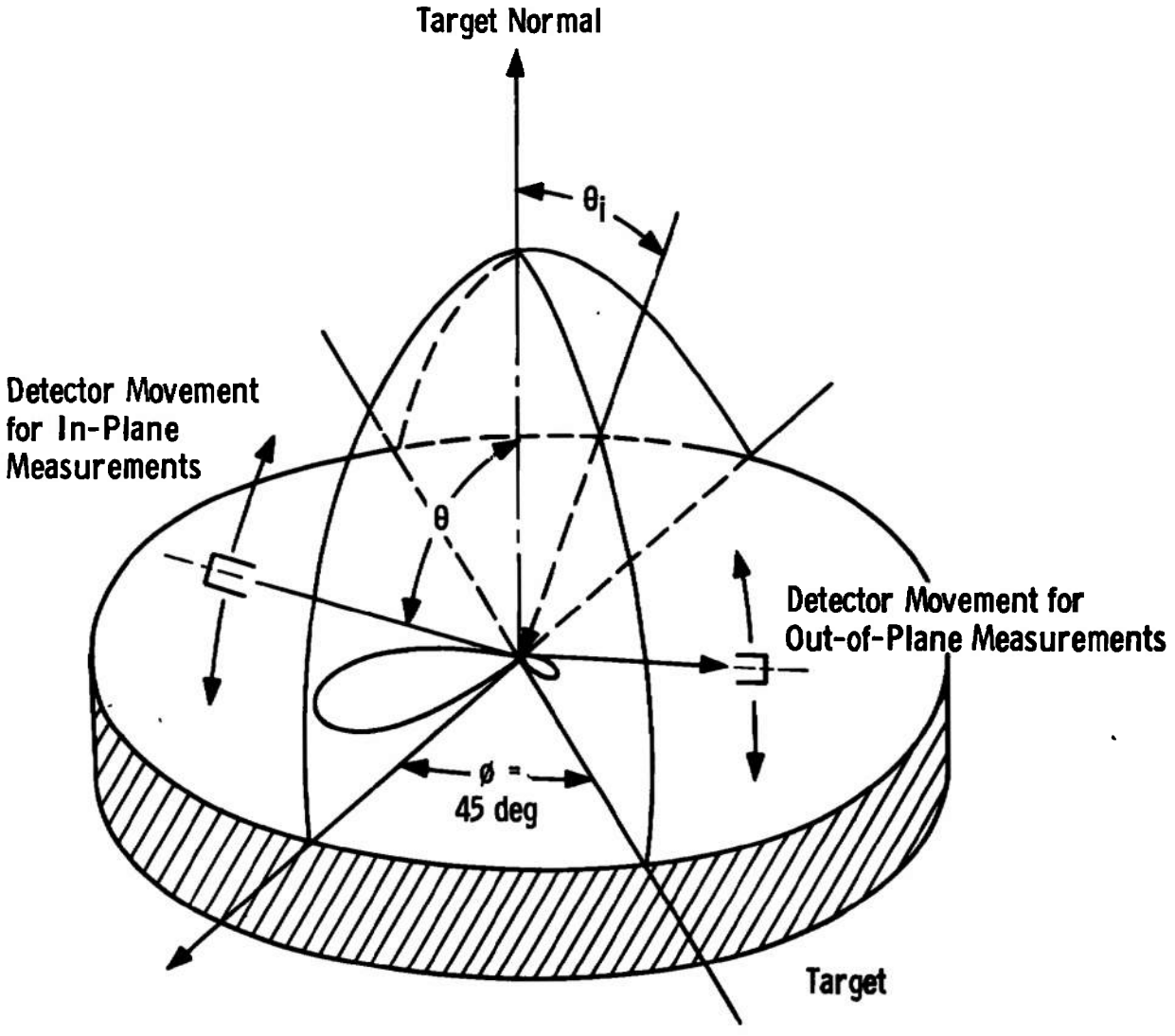

Fig. 16 Geometry for Out-of-Plane Spatial Distribution Measurements

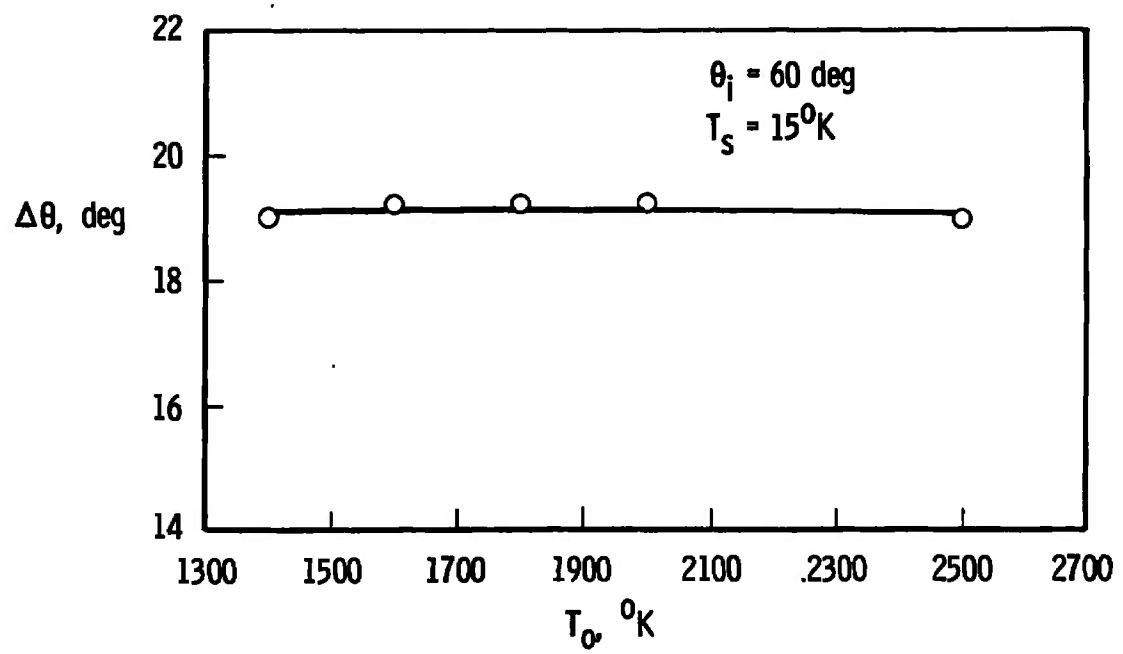

a. Variation of $\Delta\theta$ for Various Source Temperatures

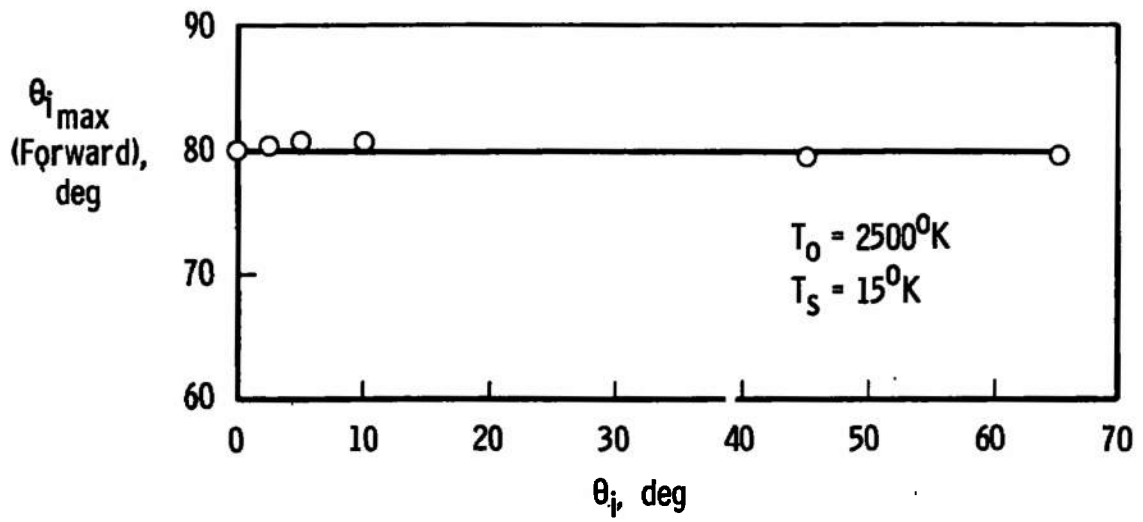

b. Variation of $\theta_{R_{max}}$ for Various Angles of Incidence

Fig. 17 Characteristic Trends of the Experimental Data

APPENDIX II
AN ESTIMATION OF THE BEAM CAPTURE COEFFICIENT FOR ARGON GAS-ARGON CRYSTAL INTERACTIONS

The beam capture coefficient has been defined previously (Ref. 15) as

$$C_b = 1 - \frac{\dot{n}_r}{\dot{n}_i}$$

where $\dot{n}_r$ is the total reflected beam flux and $\dot{n}_i$ is the total incident beam flux. If any gas is evaporating from the target surface, the magnitude of the evaporation flux can be determined by extinguishing the incident beam and recording the remaining detector signal. The reflected gas flux is

$$\dot{n}_r = \dot{n}_t - \dot{n}_v$$

where $\dot{n}_t$ is the total gas flux leaving the surface and $\dot{n}_v$ is the evaporation flux. For these experiments the surface temperature was 15°K for the argon-argon interactions and the evaporation flux was not detectable. Thus, the beam capture coefficient is

$$C_b = 1 - \frac{\dot{n}_t}{\dot{n}_i}$$

The phase-sensitive detection system responds to the number of particles per area per time and thus $\dot{n}_t$ may be determined from the relation

$$\dot{n}_t = \int_{\Omega} I(\alpha,\beta)d\Omega$$

where $I(\alpha, \beta)$ is the detector signal and $d\Omega$ is the solid angle subtended by the detector.

For large angles of incidence, the beam capture coefficient can be estimated by considering the geometry shown in Fig. II-1. The angles α and β are measured as shown in the figure. Invariance of I with respect to β is assumed. Such an assumption is perhaps justified based on the results of Section 4.1.3. Also, out-of-plane measurements of the spatial flux distributions of argon on heated platinum reveal symmetry in the β direction (Ref. 18). Thus, the total gas flux leaving the surface may be expressed as

$$\dot{n}_t = 2\pi R^2 \int_0^{\alpha_o} I(\alpha)\sin(\alpha_o - \alpha)\, d\alpha$$

where R is the radial distance from the center of the target to the detector. The total incident beam flux is determined in terms of detector

signal by considering the reflected spatial distribution of a noncondensing beam on the target surface. The experimental data in Fig. 8 show a cosine spatial flux distribution for a noncondensing argon beam on a 36°K copper surface. For such a case, $I(\alpha)$ is given by A cos α and α_o = 0 deg. The value of $\dot{n}_i$ is:

$$\dot{n}_t = 2\pi R^2 \int_0^{\frac{\pi}{2}} A \cos \alpha \sin \alpha \, d\alpha = \pi R^2 A$$

Thus, the beam capture coefficient can be expressed by:

$$C_b = 1 - \frac{2}{A} \int_0^{\alpha_o} I(\alpha) \sin (\alpha_o - \alpha) \, d\alpha$$

The integral was approximated using Simpson's rule and the corresponding values of $I(\alpha)$ for the various gas temperatures. From Fig. 8 one finds that the value of A is 3.4 mv. Figure II-2 shows the variation of the argon-argon capture coefficient with beam stagnation temperature for 60-deg angle of incidence, a 15°K surface temperature, and beam flux of 6.5×10^{15} molecules/sec.

In order to estimate the beam capture coefficient for normal beam incidence, consider the geometry shown in Fig. II-3 with α and β measured as shown. The experimental data of Fig. 10 indicate symmetry in β for $\theta_i = 0$. Thus, the total gas flux leaving the surface may be expressed as

$$\dot{n}_t = 2\pi R^2 \int_0^{\frac{\pi}{2}} I(\alpha) \sin (\alpha) \, d\alpha$$

The total incident beam flux is still

$$\dot{n}_i = \pi R^2 A.$$

Then the beam capture coefficient for normal incidence is

$$C_b = 1 - \frac{2}{A'} \int_0^{\frac{\pi}{2}} I(\alpha) \sin d\alpha$$

The integral was once again approximated using Simpson's rule and the corresponding values of $I(\alpha)$. The value of A is 5760 μv since the beam flux for this case was 1.1×10^{16} molecules/sec. One finds that the beam capture coefficient for normal beam incidence on the argon cryofrost is

$$C_b \approx 1 - 0.01 = 0.99$$

An estimation of C_b for other small angles of incidence is not possible since the spatial flux distributions do not exhibit the symmetry of the previously described cases.

Only the results of a preliminary investigation of the beam capture coefficient have been presented here. For a detailed analysis, one must have more experimental data, in particular out-of-plane and in-plane measurements of the spatial flux distributions for various angles of incidence and surface temperatures.

As shown in Fig. II-2, the argon capture coefficient decreases as the stagnation temperature or beam energy increases for a 60-deg incident angle, 15°K surface temperature, and a beam flux of 6.5×10^{15} molecules/sec. Its value varied from 0.876 at 1400°K to 0.520 at 2500°K.

The capture coefficient for normal incidence and a beam stagnation temperature of 2500°K was estimated to be 0.99. Goodman, using his n-D lattice model, has given an approximate result for the capture coefficient as a function of gas temperature for rare gas-rare gas crystal interactions (Ref. 19). He finds

$$C_b(T) \approx 1 - (1 + X)e^{-X}$$

where $X \approx \frac{2.3\epsilon}{T_g} \frac{\text{mole-deg}}{\text{cal}}$ and ϵ is the Lennard-Jones well-depth parameter. For an argon-argon crystal interaction and a beam temperature of 300°K, Goodman reports a capture coefficient of 0.58. If his formula is applied for a beam temperature of 2500°K, one finds that

$$C_b\,(2500°K) \approx 0.04$$

Goodman has assumed an incident Maxwellian beam, whereas the beam in the experiment reported here was essentially monoenergetic. On the other hand, one-dimensional lattice models would predict capture coefficients for normal incidence to be greater than 0.99 (Ref. 19). Thus, it appears from these very limited experimental results that one-dimensional lattice models predict capture coefficients in the range estimated by this report.

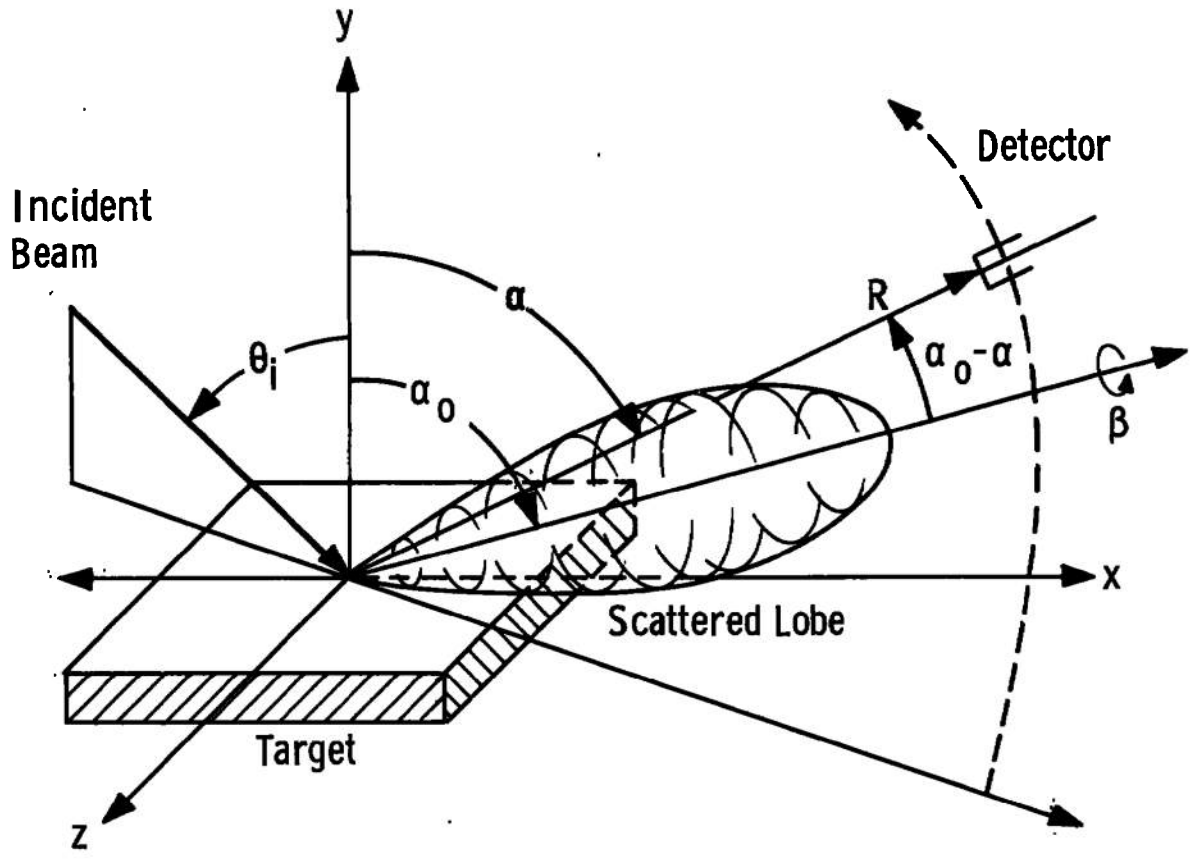

Fig. II-1 Beam Geometry for Large Angles of Incidence.

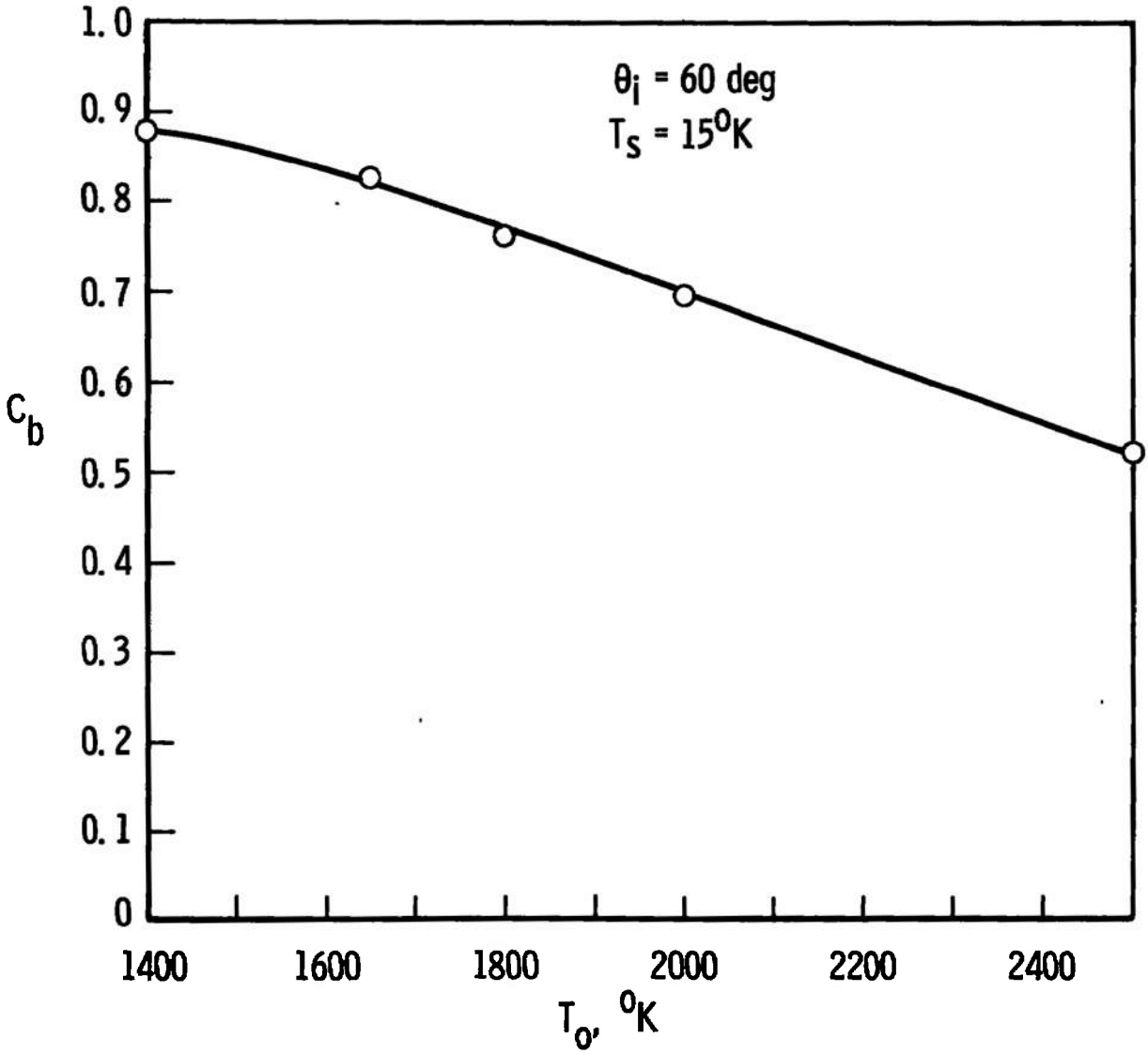

Fig. II-2 Argon-Argon Capture Coefficients for Stagnation Temperatures

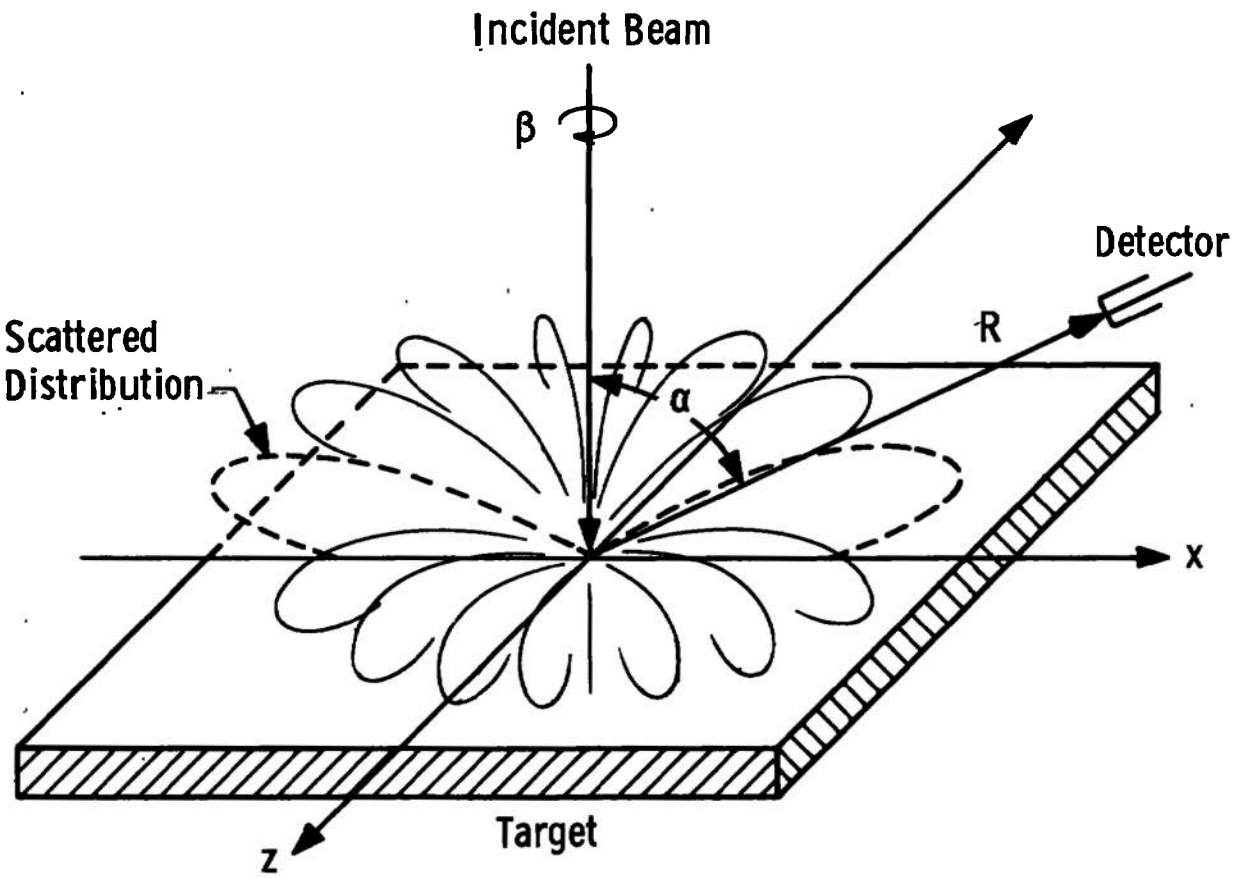

Fig. II-3 Beam Geometry for Normal Incidence

UNCLASSIFIED

Security Classification

DOCUMENT CONTROL DATA - R & D

(Security classification of title, body of abstract and indexing annotation must be entered when the overall report is classified)

1. ORIGINATING ACTIVITY (Corporate author)	2a. REPORT SECURITY CLASSIFICATION
Arnold Engineering Development Center ARO, Inc., Operating Contractor Arnold Air Force Station, Tennessee 37389	UNCLASSIFIED
	2b. GROUP N/A

3. REPORT TITLE

PRELIMINARY INVESTIGATION OF THE INTERACTION OF 0.30- TO 0.54-EV GASEOUS ARGON WITH A SOLID ARGON SURFACE

4. DESCRIPTIVE NOTES *(Type of report and inclusive dates)*

Final Report October to November 1968

5. AUTHOR(S) *(First name, middle initial, last name)*

M. R. Busby and R. F. Brown, ARO, Inc.

6. REPORT DATE	7a. TOTAL NO. OF PAGES	7b. NO. OF REFS
November 1969	44	19

8a. CONTRACT OR GRANT NO.	9a. ORIGINATOR'S REPORT NUMBER(S)
F40600-69-C-0001 b. Related to Program Element c. 61102F, Project 8951 d.	AEDC-TR-69-195
	9b. OTHER REPORT NO(S) *(Any other numbers that may be assigned this report)* N/A

10. DISTRIBUTION STATEMENT

This document has been approved for public release and sale; its distribution is unlimited.

11. SUPPLEMENTARY NOTES	12. SPONSORING MILITARY ACTIVITY
Available in DDC.	Arnold Engineering Development Center, Air Force Systems Command, Arnold AF Station, Tenn. 37389

13. ABSTRACT

An aerodynamic molecular beam and phase-sensitive detection system were used to investigate the spatial distributions of argon atoms reflected from solid argon for incident energies of from 0.30 (beam temperature of 1400°K) to 0.54 ev (beam temperature of 2500°K), incident angles from 0 to 70 deg, and solid argon temperatures of 15°K. Both in-plane and out-of-plane spatial distribution measurements were made, and highly nondiffuse supraspecular spatial flux distributions were observed for the noncondensing atoms. The angle of maximum reflected intensity was independent of both beam incident angle and beam energy. For incident angles (measured with respect to the surface normal) of 5 deg or less, "backward" reflection lobes were observed, and the magnitude of the reflected flux increased as the angle of incidence approached zero. The beam capture coefficient was a function of the incident beam energy and the angle of incidence. However, with a beam source temperature of 2500°K, the capture coefficient was near unity for normal incidence.

DD FORM 1 NOV 65 1473

UNCLASSIFIED

Security Classification

14. KEY WORDS	LINK A		LINK B		LINK C	
	ROLE	WT	ROLE	WT	ROLE	WT
argon						
particle interactions						
molecular beam						
sensing devices						
spatial distribution						
reflection						
intensity						

AFSC
Arnold AFS Tenn